

Spin-wave excitations and electron spin resonance in symmetric and asymmetric narrow-gap quantum wells

S. S. Krishtopenko and V. I. Gavrilenko*

*Institute for Physics of Microstructures RAS, Nizhny Novgorod, GSP-105, 603950 Russia*M. Goiran[†]*Laboratoire National des Champs Magnétiques Intenses (LNCMI-T), CNRS, UPR 3228 Université de Toulouse, 143 avenue de Rangueil, F-31400 Toulouse, France*

(Received 17 August 2012; revised manuscript received 13 February 2013; published 4 April 2013)

We report a theoretical study of spin-wave excitations and electron spin resonance (ESR) in a perpendicular magnetic field in *n*-type narrow-gap quantum well (QW) heterostructures. Using the Hartree-Fock approximation, based on the $8 \times 8 \mathbf{k} \cdot \mathbf{p}$ Hamiltonian, the many-body corrections to the ESR energy are found to be nonzero in symmetric and asymmetric QWs. We demonstrate a significant enhancement of the ESR energy in the asymmetric QWs, induced by the Bychkov-Rashba spin splitting and exchange interaction in weak and moderate magnetic fields, as well as the exchange-induced divergence of the ESR *g* factor in the symmetric QWs in weak magnetic fields. We calculate the spin-wave dispersions at odd-valued filling factors of the Landau levels for different values of 2D electron concentration in the symmetric and asymmetric InAs/AlSb QW heterostructures. We predict a gap for the long wavelength spin-wave excitations in symmetric and asymmetric narrow-gap QWs induced by the spin-orbit interaction and subband nonparabolicity. The many-body renormalization of electron spin resonance energies in HgTe/CdHgTe QWs is also qualitatively discussed.

DOI: [10.1103/PhysRevB.87.155113](https://doi.org/10.1103/PhysRevB.87.155113)

PACS number(s): 73.21.Fg, 73.43.Lp, 73.61.Ey, 75.30.Ds

I. INTRODUCTION

A simplest neutral excitation in a 2D electron gas (2DEG) placed in a perpendicular magnetic field is a *spin wave* (or *spin exciton*) arising at the electron transition between the Landau levels (LLs) spin-split through Zeeman interaction. This type of excitation was first studied theoretically by Kallin and Halperin.¹ They employed a diagrammatic approach for the Coulomb interaction between the electrons at integer-valued filling factors of LLs. Later, the theory of Kallin and Halperin was elaborated by taking into account the disorder broadening of the LLs within the self-consistent Born approximation.²

Longo and Kallin³ studied spin-wave (SW) excitations in the fractional quantum Hall effect (FQHE) regime. By using the single-mode approximation (SMA), they have calculated the SW dispersions for the small wavelengths up to the magnetic length. Subsequently, Nakajima and Aoki⁴ have performed the calculations of SW excitations of FQHE system at $\nu = 1/3$ and $1/5$ for to wavelength exceeding the magnetic length. They started from the results of Kallin and Halperin for the 2DEG at $\nu = 1$ turned to the spherical geometry approach, introduced the composite-fermion picture,⁵ and then performed mean-field calculations. The results of Nakajima and Aoki for $\nu = 1/3$ have been also reproduced by Murthy, who developed the dynamical theory of composite fermions.⁶ Finally, Mandal⁷ studied the SW excitations for arbitrarily polarized FQHE states by employing a fermionic Chern-Simons gauge theory in the low Zeeman energy limit.

We note that the theoretical results obtained have already been confirmed by numerous experiments on inelastic light scattering⁸ used to study SW excitations in GaAs quantum wells (QWs). The common feature reported in the above papers^{1-4,6,7} is that the single-particle LLs in magnetic field were described by a 2×2 Hamiltonian that contains only the

effective mass m^* and the *g* factor g^* as phenomenological parameters:

$$E_{n,\sigma_z} = \hbar\omega_c (n + 1/2) + \mu_B g^* B \sigma_z, \quad (1)$$

where $\omega_c = eB/m^*c$, m^* is the electron effective mass, c is the light velocity, and μ_B is the Bohr magneton. We would like to note that this approximation is valid for QW heterostructures with the parabolic energy-momentum law in the electronic subbands only.

The long-wavelength limit of SW excitations is observed in the electron spin resonance (ESR). In 2DEG with rotational invariance, in the spin space, the Larmor theorem dictates that Coulomb interactions do not contribute in the ESR energy. In systems with the LLs described by Eq. (1), the Larmor theorem is valid.⁹⁻¹² *Spin-orbit interaction* (SOI) perturbs the spin invariance in 2DEG, which results in violation of the Larmor theorem. To date, only one paper¹³ has reported theoretical evidence of an SOI-induced breaking of the Larmor theorem in 2DEG. They investigated the effect of the SOI induced Bychkov-Rashba (BR) term¹⁴ on the zero-momentum SWs in 2DEG in the FQHE regime.

Typical narrow-gap QW heterostructures based on InSb¹⁵⁻¹⁸ and InAs¹⁹⁻²³ are characterized by pronounced *nonparabolicity* of the electronic subbands, experimentally observed in the cyclotron resonance (CR) studies.¹⁵⁻²³ Besides, these structures feature strong SOI related effects.²⁴⁻²⁹ Pfeffer and Zawadzki³⁰⁻³² were the first to have studied in details the changes induced in the Bychkov-Rashba¹⁴ and Dresselhaus³³ contributions in spin splitting by the nonparabolicity, in particular. A nonlinear dependence of the spin splitting on quasimomentum in a zero-magnetic field was demonstrated. Therefore, to correctly account for the SW excitations in narrow-gap QWs, both the nonparabolicity and SOI should be taken into consideration.

One typical representative of the narrow-gap 2D systems is the InAs/AlSb QW heterostructures.^{19–23,34–37} They are characterized by small values of the effective electron mass in the InAs QW,²¹ high values of the g factor,³⁴ and high mobility of 2D electrons.³⁵ Investigations of CR in the InAs/AlSb heterostructures revealed a strong dependence of the cyclotron mass on 2DEG concentration due to subband nonparabolicity.^{19–23} It is a well-known fact that even nominally undoped InAs/AlSb structures contain a 2DEG in the concentration of the order of 10^{12} cm⁻² (see Refs. 21 and 34–37). These electrons are more likely supplied from the deep donors related to defects in AlSb, and the surface donors in the GaSb cap layer that is typically grown over the AlSb barrier to protect it from air oxidation.^{36,37} The electric field of spatially separated donors in the GaSb cap layer and of 2D electrons causes distortion of the QW potential, which, in turn, leads via SOI to the BR splitting of 2DEG spectrum in InAs/AlSb QW in zero magnetic field.^{27–29} A notable feature of InAs/AlSb QW heterostructures is the effect of bipolar persistent photoconductivity (PPC) that is observable at low temperatures.^{37–40} It offers the possibility to change an asymmetry of the “built-in” electric field and the BR splitting values via sample illumination with LEDs of appropriate wavelengths.^{38,40}

To describe the single-electron states in the conduction band Γ_6 in such n -type narrow-gap QWs, we first start from the 8×8 $\mathbf{k}\cdot\mathbf{p}$ Hamiltonian⁴¹ with the kinetic part for the conduction band in the form proposed by Foreman⁴² and then neglect the terms resulting from remote band contributions. Note that in this case, the interband momentum matrix element P should also be normalized to fit conduction band mass m_c .⁴¹ This procedure is described in details in Ref. 42. Below we advance the arguments confirming the validity of such approximation for the n -type QWs based on InAs and InSb. A similar approach was also used by Winkler^{43,44} to explain the experiments on CR in InAs/AlSb QWs performed by Yang *et al.*¹⁹ and Scriba *et al.*⁴⁵ There was a good agreement between Winkler’s calculation and the experimental data. We have also employed this approximation for a quantitative interpretation of our previous experimental results on CR^{22,23} and magnetotransport²⁹ in InAs/AlSb QWs. Moreover, it can be shown that our approximation for the single-particle states can be reduced to the model proposed by Pfeffer and Zawadzki⁴⁶ for the spin splitting in the conduction band in n -type QWs based on narrow-gap materials.

Our earlier studies^{29,47–50} have shown the nonparabolicity of electronic subbands resulted from the mixing of Γ_6 band with the bands Γ_7 and Γ_8 to largely influence the electron-electron (e-e) interaction effects in 2DEG. In Refs. 29, 47, 48, and 50, a detailed theory of the exchange enhancement of the quasiparticle g factor in narrow-gap QWs was proposed. It was demonstrated that the nonparabolicity leads to exchange enhancement of the quasiparticle g factor for *any* filling factors of the LLs in the InAs/AlSb QWs in contrast to the QWs with parabolic electronic subbands, which were the first studied by Ando and Uemura.⁵¹ Recently, we have provided a first theoretical evidence of the Larmor theorem violation in symmetric narrow-gap QWs.⁴⁹ We have shown that the ESR and quasiparticle g factors, measured in magnetotransport, coincide at *even-valued* filling factors of the LLs in moderate and

quantizing magnetic fields. The latter paper⁵² demonstrates a Larmor theorem violation for fractional quantum Hall states in symmetric n -type QWs based on narrow-gap materials.

In this paper, we extend the limits of our previous works^{49,52} to a theoretical study of the SW excitations and ESR in the InAs/AlSb QWs with symmetric and asymmetric potential profiles. Using the Hartree-Fock approximation based on the 8×8 $\mathbf{k}\cdot\mathbf{p}$ Hamiltonian⁴¹ included the mixing of the conduction and valence bands, we directly take into account the influence of nonparabolicity, lattice deformation and SOI on the electronic subbands. Since the SOI is inherent in the 8×8 $\mathbf{k}\cdot\mathbf{p}$ Hamiltonian, narrow-gap QWs it describes do not feature rotation invariance in the spin space. The latter circumstance is supposed to cause the Larmor theorem violation in narrow-gap QWs. In the paper, we consider the dominant Bychkov-Rashba contribution in the spin splitting induced by the structure inversion asymmetry (SIA), since the Dresselhaus terms in narrow-gap QWs are small.^{53,54}

The paper is organized as follows. The general theory in terms of excitonic representation for SW excitations in narrow-gap QWs is described in Sec. II. Calculations of the ESR energies, g factors, and the SW dispersions for different values of the 2DEG concentration and magnetic fields in the InAs/AlSb QW heterostructures are performed in Sec. III. The main results of this work are summarized in Sec. IV.

II. THE FORMALISM

The total Hamiltonian of 2DEG in the second quantized representation has the form:

$$\begin{aligned}\hat{H} &= \hat{H}_0 + \hat{H}_{\text{int}}, \\ \hat{H}_0 &= \int_{-\infty}^{+\infty} dz \int d^2\vec{r} \hat{\Psi}^+(\vec{r}, z) \hat{H}_{(1e)} \hat{\Psi}(\vec{r}, z), \\ \hat{H}_{\text{int}} &= \frac{1}{2} \int_{-\infty}^{+\infty} dz_1 \int_{-\infty}^{+\infty} dz_2 \int d^2\vec{r}_1 \int d^2\vec{r}_2 \hat{\Psi}^+(\vec{r}_1, z_1) \\ &\quad \times \hat{\Psi}^+(\vec{r}_2, z_2) V(|\vec{r}_1 - \vec{r}_2|, z_1, z_2) \hat{\Psi}(\vec{r}_2, z_2) \hat{\Psi}(\vec{r}_1, z_1),\end{aligned}\tag{2}$$

where \hat{H}_0 is the Hamiltonian of single-electron states in a quantum well, $V(|\vec{r}_1 - \vec{r}_2|, z_1, z_2)$ is the Coulomb Green function in a three-layer medium,⁴⁷ describing the interaction of two charges at points (\vec{r}_1, z_1) and (\vec{r}_2, z_2) , and \vec{r} is the vector lying in the QW plane, axis z is perpendicular to the QW plane.

In Eq. (2), we have introduced the field operators $\hat{\Psi}(\vec{r}, z)$ and $\hat{\Psi}^+(\vec{r}, z)$ defined by the fermion creation and annihilation operators $a_{n,k,i}$ and $a_{n,k,i}^+$, respectively, and by the single-electron wave functions $\Psi_{n,k}^{(i)}(\vec{r}, z)$ of Hamiltonian $\hat{H}_{(1e)}$:

$$\begin{aligned}\hat{\Psi}(\vec{r}, z) &= \sum_{n,k,i} \Psi_{n,k}^{(i)}(\vec{r}, z) a_{n,k,i}, \\ \hat{\Psi}^+(\vec{r}, z) &= \sum_{n,k,i} (\Psi_{n,k}^{(i)}(\vec{r}, z))^+ a_{n,k,i}^+, \end{aligned}\tag{3}$$

where the upper sign “+” denotes the Hermitian conjugation.

A. Single-electron problem: Summary

As mentioned in Introduction, all calculations in this work are performed for the narrow-gap InAs/AlSb QW heterostructures with the GaSb cap layer. To correctly account

for the influence of nonparabolicity caused by mixing of the conduction band (Γ_6) with the valence bands (Γ_7 and Γ_8), and of SOI on the single-electron states in narrow-gap QWs, we use the eight-band $\mathbf{k}\cdot\mathbf{p}$ Hamiltonian⁴¹ as a single-particle operator for the kinetic energy. Note that the Hamiltonian can be *simplified* to describe the conduction band states in n -type narrow-gap QWs based on InAs and InSb by neglecting the terms resulting from the remote band contribution.⁴⁷

By taking into account the arguments from Ref. 47, in a given basis of the Bloch functions at Γ point of the Brillouin zone,⁴¹ with the terms associated with the absence of the inversion center in an elementary cell of bulk materials^{31,32} and with low-symmetry interfaces⁵⁵ being neglected, the eight-band $\mathbf{k}\cdot\mathbf{p}$ Hamiltonian takes the form

$$H_{8\times 8}^{\vec{k},\vec{p}} = H_{b,b^+} + H_Z + H_\varepsilon, \quad (4)$$

where H_{b,b^+} has the following form:

$$H_{b,b^+} = \begin{pmatrix} H_{CC} & H_{CH} \\ H_{CH}^+ & H_{HH} \end{pmatrix}, \quad (5)$$

$$H_{HH} = \begin{pmatrix} E_v & 0 & 0 & 0 & 0 & 0 \\ 0 & E_v & 0 & 0 & 0 & 0 \\ 0 & 0 & E_v & 0 & 0 & 0 \\ 0 & 0 & 0 & E_v & 0 & 0 \\ 0 & 0 & 0 & 0 & E_v - \Delta & 0 \\ 0 & 0 & 0 & 0 & 0 & E_v - \Delta \end{pmatrix},$$

$$H_{CC} = \begin{pmatrix} E_c & 0 \\ 0 & E_c \end{pmatrix}, \quad H_{CH}^+ = \begin{pmatrix} -\frac{Pb}{a_B} & 0 \\ \frac{\{Pk_z\}}{\sqrt{6}} & -\frac{Pb}{\sqrt{3}a_B} \\ \frac{Pb^+}{\sqrt{3}a_B} & \frac{\{Pk_z\}}{\sqrt{6}} \\ 0 & \frac{Pb^+}{a_B} \\ -\frac{\{Pk_z\}}{2\sqrt{3}} & -\sqrt{\frac{2}{3}}\frac{Pb}{a_B} \\ -\sqrt{\frac{2}{3}}\frac{Pb^+}{a_B} & \frac{\{Pk_z\}}{2\sqrt{3}} \end{pmatrix}$$

Here, $\{A,B\} = AB + BA$ is the anticommutator for the operators A and B , P is the Kane momentum matrix element, $E_c(z)$ and $E_v(z)$ are the conduction- and valence-band edges, respectively, $\Delta(z)$ is the SOI energy, b^+ and b are the ladder operators,⁴⁷ and $k_z = -i\frac{\partial}{\partial z}$. Further, we assume that the magnetic field is oriented along z axis, and the z axis coincides with the crystallographic direction (001); the x and y axes correspond to directions (100) and (010), respectively. In the 8×8 $\mathbf{k}\cdot\mathbf{p}$ Hamiltonian (4), H_Z contains the terms describing the Zeeman splitting in a magnetic field and H_ε defines the influence of the lattice-mismatch strain on single-electron energies.

The misalignment of energy band gaps in adjacent layers of the heterostructure is taken into account by defining a band offset function relative to the InAs QW layer. This potential energy given by $\Delta(\text{VBO}) = \text{VBO}_{\text{AlSb}} - \text{VBO}_{\text{InAs}}$ defines the band edge profile $E_v(z)$ for the top of the valence band. Valence-band offsets VBO_{InAs} and VBO_{AlSb} are determined experimentally.⁵⁶ Counting the energy from conduction-band bottom in unstrained bulk InAs, the valence band edge $E_v(z)$ in InAs/AlSb QW is defined as follows:

$$E_v(z) = \begin{cases} -E_{g,\text{InAs}}, & 0 \leq z \leq d, \\ -E_{g,\text{InAs}} + \Delta(\text{VBO}), & z < 0 \text{ or } z > d, \end{cases}$$

where d is a QW width and $E_{g,\text{InAs}}$ corresponds to the band-gap energy in InAs. The conduction-band edge is defined by $E_c(z) = E_v(z) + E_g(z)$. The values for VBO_{InAs} and VBO_{AlSb} are given in Ref. 56.

In this paper, the InAs/AlSb QW heterostructures are considered to be grown on the [001] plane,^{19–23} which means that the strain tensor can have only three nonzero components: $\varepsilon_{xx} = \varepsilon_{yy}$, ε_{zz} . From the condition of zero external stress along the (001) direction, we can get the relation between ε_{xx} and ε_{zz} :

$$\varepsilon_{xx} = \varepsilon_{yy} = \frac{a_0 - a}{a}, \quad \varepsilon_{zz} = -\frac{2C_{12}}{C_{11}}\varepsilon_{xx},$$

where C_{ij} are the elastic constants in each layer, a and a_0 are the lattice constants of the given layer and the unstrained AlSb barriers, respectively. The explicit form of H_ε , can be easily obtained from Eq. (C3) in Ref. 41.

The Zeeman term H_Z in Eq. (4) in the Bloch function basis of this paper is the following matrix:

$$H_Z = \hbar \frac{eB}{m_0c} \begin{pmatrix} H_{CC}^{(Z)} & 0 \\ 0 & H_{HH}^{(Z)} \end{pmatrix}, \quad (6)$$

with

$$H_{CC}^{(Z)} = \begin{pmatrix} \frac{g^*}{4} & 0 \\ 0 & -\frac{g^*}{4} \end{pmatrix},$$

$$H_{HH}^{(Z)} = \begin{pmatrix} -\frac{3}{2}\kappa & 0 & 0 & 0 & 0 & 0 \\ 0 & -\frac{1}{2}\kappa & 0 & 0 & -\frac{\kappa+1}{\sqrt{2}} & 0 \\ 0 & 0 & \frac{1}{2}\kappa & 0 & 0 & -\frac{\kappa+1}{\sqrt{2}} \\ 0 & 0 & 0 & \frac{3}{2}\kappa & 0 & 0 \\ 0 & -\frac{\kappa+1}{\sqrt{2}} & 0 & 0 & -(\kappa + \frac{1}{2}) & 0 \\ 0 & 0 & -\frac{\kappa+1}{\sqrt{2}} & 0 & 0 & \kappa + \frac{1}{2} \end{pmatrix},$$

where m_0 is the free-electron mass, c is the light velocity, and B is a magnetic-field straight. As we have ignored the coupling with the remote bands, not included in the eight-band $\mathbf{k}\cdot\mathbf{p}$ Hamiltonian, we have set the modified Luttinger parameters $\gamma_1, \gamma_2, \gamma_3$ equal to zero, as a result P, g^* , and κ are expressed as follows:⁴⁷

$$P^2 = \frac{3\hbar^2}{2m_c} \frac{E_g(E_g + \Delta)}{3E_g + 2\Delta},$$

$$g^* = g_c + \frac{m_0}{m_c} \frac{2\Delta}{3E_g + 2\Delta},$$

$$\kappa = -\frac{2}{3},$$

where m_c and g_c are the conduction band effective mass and g factor, respectively.

In order to find a “built-in” electric field, distorting the QW profile and leading to the Bychkov-Rashba effect,²⁸ it is necessary to include in the Hamiltonian $\hat{H}_{(1e)}$ for the single-particle states, not only the electric field of ionized donors in the AlSb barriers and in the GaSb cap layer $V_{\text{donors}}(z)$, but the local part of the Coulomb energy (Hartree potential)⁴⁸ $-e\varphi_{e-e}$

as well:

$$\hat{H}_{(1e)} = H_{8 \times 8}^{\vec{k}, \vec{p}} + V_{\text{donors}}(z) - e\varphi_{e-e}, \quad (7)$$

where $e > 0$ is the elementary charge. The term $V_{\text{donors}}(z)$ can be easily obtained from the following equation:

$$\epsilon(z) \frac{\partial V_{\text{donors}}(z)}{\partial z} = 2\pi e^2 (n_L - n_R), \quad (8)$$

with conditions

$$\begin{aligned} V_{\text{donors}}(z-0) &= V_{\text{donors}}(z+0) = 0, \\ V_{\text{donors}}(d-0) &= V_{\text{donors}}(d+0), \end{aligned} \quad (9)$$

where $\epsilon(z)$ is the permittivity in each layer of the heterostructure, n_L is the ionized donor concentration in the GaSb cap layer and the top barrier, and n_R corresponds to the donor concentration in the bottom AISb barrier far from the QW. We note that according to the neutrality principle $n_L + n_R = n_S$, where n_S is a 2DEG concentration.

To calculate the Hartree potential $-e\varphi_{e-e}$, one should solve the set of Poisson and Schrödinger equations:

$$\begin{aligned} \frac{\partial}{\partial z} \left(\epsilon \frac{\partial \varphi_{e-e}}{\partial z} \right) &= 4\pi e \sum_{n', i'} \frac{v_{n'}^{(i')}}{2\pi a_B^2} \sum_{p=1}^8 |c_p^{(i')}(z, n')|^2, \\ \hat{H}_{(1e)} \Psi_{n,k}^{(i)}(\vec{r}, z) &= E_n^{(i)} \Psi_{n,k}^{(i)}(\vec{r}, z). \end{aligned} \quad (10)$$

By taking the Landau gauge for the vector potential,^{41,47,48} the eight-component wave function $\Psi_{n,k}^{(i)}(\vec{r}, z)$ of $\hat{H}_{(1e)}$, being defined by the normalized harmonic oscillator functions $|n, k\rangle$, can be written as follows:⁴⁷

$$\Psi_{n,k}^{(i)}(\vec{r}, z) = \begin{pmatrix} c_1^{(i)}(z, n) |n, k\rangle \\ c_2^{(i)}(z, n) |n+1, k\rangle \\ c_3^{(i)}(z, n) |n-1, k\rangle \\ c_4^{(i)}(z, n) |n, k\rangle \\ c_5^{(i)}(z, n) |n+1, k\rangle \\ c_6^{(i)}(z, n) |n+2, k\rangle \\ c_7^{(i)}(z, n) |n, k\rangle \\ c_8^{(i)}(z, n) |n+1, k\rangle \end{pmatrix}, \quad (11)$$

where n is the LL index, i is the ‘‘spin’’ index, and k is the parameter for the degenerate states within the same LL in the Landau gauge. In this paper, we focus on QWs with a single occupied subband, therefore, the index labeling the electronic subbands is omitted.

For $n = -1$, there is only one four-component eigenfunction of Hamiltonian $\hat{H}_{(1e)}$:

$$\Psi_{-1,k}^{(b)}(\vec{r}, z) = \begin{pmatrix} 0 \\ c_2^{(b)}(z, -1) |0, k\rangle \\ 0 \\ 0 \\ c_5^{(b)}(z, -1) |0, k\rangle \\ c_6^{(b)}(z, -1) |1, k\rangle \\ 0 \\ c_8^{(b)}(z, -1) |0, k\rangle \end{pmatrix}, \quad (12)$$

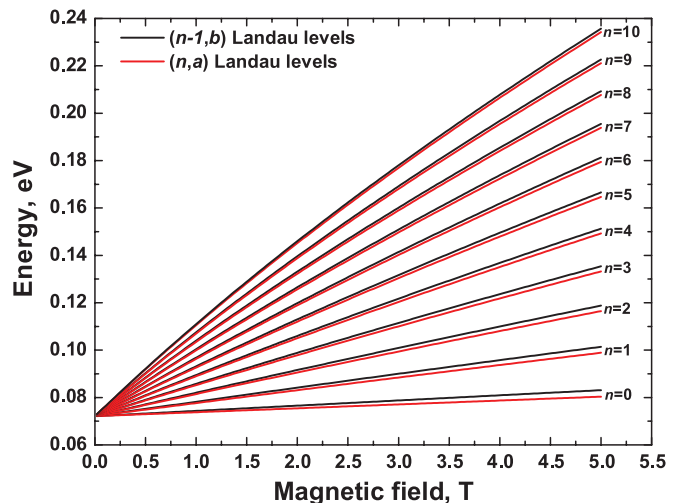


FIG. 1. (Color online) Landau levels (n, i) in the first electronic subband in a 15-nm-wide rectangular InAs/AISb QW without a ‘‘built-in’’ electric field. The energy is counted from the conduction band bottom in unstrained bulk InAs.

At $n = 0$ (as in the case $n > 0$), the solutions of a single-particle Schrödinger equation are two wave functions:

$$\Psi_{0,k}^{(a,b)}(\vec{r}, z) = \begin{pmatrix} c_1^{(a,b)}(z, 0) |0, k\rangle \\ c_2^{(a,b)}(z, 0) |1, k\rangle \\ 0 \\ c_4^{(a,b)}(z, 0) |0, k\rangle \\ c_5^{(a,b)}(z, 0) |1, k\rangle \\ c_6^{(a,b)}(z, 0) |2, k\rangle \\ c_7^{(a,b)}(z, 0) |0, k\rangle \\ c_8^{(a,b)}(z, 0) |1, k\rangle \end{pmatrix}; \quad (13)$$

the one that corresponds to the lower single-electron energy is labeled by index a , that for the higher energy is marked by b (see Fig. 1). Note that by using eight-component wave functions for single-electron states, we directly take into account the influence of the mixing between the conduction and valence bands on the matrix elements of e-e interaction, which plays a principle role in many-body effects in narrow-gap QWs.^{47–50,52}

B. Excitonic representation

The spectra of various collective excitations can be readily calculated using the means of exciton representation.^{57–63} The simplest kinds of excitation in the system, such as a *cyclotron magnetoplasmon*^{1,59,62} (Refs. 1,41,44) and a *spin wave*^{1,60,63} can be regarded as excitation of magnetic excitons formed by an electron that excited onto an unfilled or partially filled LL (n, i) , and an effective hole appearing simultaneously at the electron’s former level (n', i') . Let us introduce the exciton creation operator^{59,62}

$$A_{n,n',i,i'}^+(\vec{k}) = \sum_p e^{ik_x(p+k_y/2)a_B^2} a_{n,p,i}^+ a_{n',p+k_y,i'} \quad (14)$$

that satisfies the following commutation relation:

$$\begin{aligned} & [A_{n_1, n_2, i_1, i_2}^+(\vec{k}_1), A_{n_3, n_4, i_3, i_4}^+(\vec{k}_2)] \\ &= e^{-\frac{i}{2}a_B^2[\vec{k}_1 \times \vec{k}_2]_z} A_{n_1, n_4, i_1, i_4}^+(\vec{k}_1 + \vec{k}_2) \delta_{n_2, n_3} \delta_{i_2, i_3} \\ &\quad - \delta_{n_1, n_4} \delta_{i_1, i_4} e^{\frac{i}{2}a_B^2[\vec{k}_1 \times \vec{k}_2]_z} A_{n_3, n_2, i_3, i_2}^+(\vec{k}_1 + \vec{k}_2), \end{aligned} \quad (15)$$

where a_B is the magnetic length ($a_B^2 = \hbar c/eB$).

The excitation energy $E_{\text{ex}}(\vec{k})$ with respect to the energy of the ground state $|0\rangle$ is found from equation

$$E_{\text{ex}}(\vec{k}) A_{n, n', i, i'}^+(\vec{k})|0\rangle = [\hat{H}, A_{n, n', i, i'}^+(\vec{k})]|0\rangle. \quad (16)$$

It can be shown that

$$E_{\text{ex}}(\vec{k}) = E_n^{(i)} - E_{n'}^{(i')} + \Delta_{\text{ex}}^{(e-e)}(\vec{k}), \quad (17)$$

where $E_n^{(i)}$ is the corresponding LL energy characterized by the spin i and LL n indices, and the contribution by the e-e interaction is determined from the following equation:

$$\Delta_{\text{ex}}^{(e-e)}(\vec{k}) A_{n, n', i, i'}^+(\vec{k})|0\rangle = [\hat{H}_{\text{int}}, A_{n, n', i, i'}^+(\vec{k})]|0\rangle. \quad (18)$$

Using the Fourier transform for the Coulomb Green function:

$$V(|\vec{r}_1 - \vec{r}_2|, z_1, z_2) = \int \frac{d^2\vec{q}}{(2\pi)^2} \tilde{D}(q, z_1, z_2) e^{i\vec{q}(\vec{r}_1 - \vec{r}_2)}, \quad (19)$$

allows one to reduce the calculations of the Coulomb potential matrix elements via the wave functions of Hamiltonian $\hat{H}_{(1e)}$ in the estimation of matrix elements $\langle n_1, k_1 | e^{i\vec{q}\vec{r}} | n_2, k_2 \rangle$.⁴⁷⁻⁴⁹

By way of simple calculations, we then arrive at the following expression for \hat{H}_{int} :

$$\begin{aligned} & \hat{H}_{\text{int}} \\ &= \frac{1}{2} \sum_{\substack{n_1 \dots n_4 \\ i_1 \dots i_4}} \int \frac{d^2\vec{q}}{(2\pi)^2} \tilde{V}_{n_1, n_2, n_3, n_4}^{(i_1, i_2, i_3, i_4)}(\vec{q}) A_{n_1, n_4, i_1, i_4}^+(\vec{q}) A_{n_2, n_3, i_2, i_3}^+(-\vec{q}) \\ &\quad - \frac{1}{2} \sum_{\substack{n_1, n_2, n_3 \\ i_1, i_2, i_3}} \int \frac{d^2\vec{q}}{(2\pi)^2} \tilde{V}_{n_1, n_2, n_2, n_3}^{(i_1, i_2, i_2, i_3)}(\vec{q}) A_{n_1, n_3, i_1, i_3}^+(0), \end{aligned} \quad (20)$$

where the matrix element $\tilde{V}_{n_1, n_2, n_2, n_3}^{(i_1, i_2, i_3, i_4)}(\vec{q})$ is defined as

$$\begin{aligned} \tilde{V}_{n_1, n_2, n_3, n_4}^{(i_1, i_2, i_3, i_4)}(\vec{q}) &= \int_{-\infty}^{+\infty} dz_1 \int_{-\infty}^{+\infty} dz_2 \tilde{D}(q, z_1, z_2) e^{-q^2 a_B^2 / 2} \\ &\quad \times \tilde{G}_{n_1, n_4}^{(i_1, i_4)}(\vec{q}, z_1, z_1) \tilde{G}_{n_2, n_3}^{(i_2, i_3)}(-\vec{q}, z_2, z_2), \end{aligned} \quad (21)$$

with $\tilde{G}_{n_1, n_2}^{(i_1, i_2)}(\vec{q}, z, z)$ in the form

$$\begin{aligned} \tilde{G}_{n_1, n_2}^{(i_1, i_2)}(\vec{q}, z, z) &= \tilde{L}_{n_1, n_2}^{(i_1, i_2)}\left(\frac{q^2 a_B^2}{2}, z, z\right) \\ &\quad \times \begin{cases} \left[\frac{(iq_x + q_y)a_B}{\sqrt{2}}\right]^{n_1 - n_2}, & n_1 \geq n_2, \\ \left[\frac{(iq_x - q_y)a_B}{\sqrt{2}}\right]^{n_2 - n_1}, & n_1 < n_2. \end{cases} \end{aligned} \quad (22)$$

In Eq. (22), $\tilde{L}_{n, n'}^{(i, i')}(x, z, z)$ is determined by the wave functions $\Psi_{n, k}^{(i)}(\vec{r}, z)$ and has the form

$$\begin{aligned} \tilde{L}_{n, n'}^{(i, i')}(x, z, z') &= \sum_{m=1, 4, 7} c_m^{(i)}(z, n) c_m^{(i')}(z', n') \sqrt{\frac{\tilde{n}_1!}{\tilde{n}_2!}} L_{\tilde{n}_1}^{\tilde{n}_2 - \tilde{n}_1}(x) + \sum_{m=2, 5, 8} c_m^{(i)}(z, n) c_m^{(i')}(z', n') \sqrt{\frac{(\tilde{n}_1 + 1)!}{(\tilde{n}_2 + 1)!}} L_{\tilde{n}_1 + 1}^{\tilde{n}_2 - \tilde{n}_1}(x) \\ &\quad + c_3^{(i)}(z, n) c_3^{(i')}(z', n') \sqrt{\frac{(\tilde{n}_1 - 1)!}{(\tilde{n}_2 - 1)!}} L_{\tilde{n}_1 - 1}^{\tilde{n}_2 - \tilde{n}_1}(x) + c_6^{(i)}(z, n) c_6^{(i')}(z', n') \sqrt{\frac{(\tilde{n}_1 + 2)!}{(\tilde{n}_2 + 2)!}} L_{\tilde{n}_1 + 2}^{\tilde{n}_2 - \tilde{n}_1}(x), \end{aligned} \quad (23)$$

where $L_m^n(x)$ are the associated Laguerre polynomials, $q = \sqrt{q_x^2 + q_y^2}$, the exponent “*” denotes the complex conjugation and $\tilde{n}_1 = \min(n, n')$, $\tilde{n}_2 = \max(n, n')$.

Now using the commutation relations (15) for the exciton creation operators, we derive the following expression for the commutator in the right-hand part of Eq. (18):

$$\begin{aligned} [\hat{H}_{\text{int}}, A_{n, n', i, i'}^+(\vec{k})] &= \sum_{\substack{n_1, n_2, n_4 \\ i_1, i_2, i_4}} \int \frac{d^2\vec{q}}{(2\pi)^2} \tilde{V}_{n_1, n_2, n_4}^{(i_1, i_2, i_4)}(\vec{q}) e^{\frac{i}{2}a_B^2[\vec{q} \times \vec{k}]_z} A_{n_2, n', i_2, i'}^+(\vec{k} - \vec{q}) A_{n_1, n_4, i_1, i_4}^+(\vec{q}) - \sum_{\substack{n_1, n_2, n_4 \\ i_1, i_2, i_4}} \int \frac{d^2\vec{q}}{(2\pi)^2} \tilde{V}_{n_1, n', n_2, n_4}^{(i_1, i', i_2, i_4)}(\vec{q}) \\ &\quad \times e^{-\frac{i}{2}a_B^2[\vec{q} \times \vec{k}]_z} A_{n_1, n_4, i_1, i_4}^+(\vec{q}) A_{n, n_2, i, i_2}^+(\vec{k} - \vec{q}). \end{aligned} \quad (24)$$

If we consider the Coulomb interaction only in the first-order approximation, of all the terms in Eq. (24) we should take into account just those containing one creation and one annihilation operator, multiplied by the operator for the number of particles. This method is fully equivalent to the approach developed by Kallin and Halperin¹ that is based on a diagrammatic representation. Following the standard rule

$$\langle 0 | a_{n_1, k_1, i_1} a_{n_2, k_2, i_2}^+ | 0 \rangle = v_{n_1}^{(i_1)} \delta_{n_1, n_2} \delta_{p_1, p_2} \delta_{i_1, i_2}, \quad (25)$$

where $v_n^{(i)}$ is the filling factor for LL (n, i) , after rather tedious mathematical transformations, we obtain the following expression for commutator $[\hat{H}_{\text{int}}, A_{n,n',i,i'}^+(\vec{k})]$:

$$[\hat{H}_{\text{int}}, A_{n,n',i,i'}^+(\vec{k})]|0\rangle = \sum_{n_2, i_2} v_{n_2}^{(i_2)} \left(\frac{\tilde{V}_{n, n_2, n_2, n}^{(i, i_2, i_2, i)}(0)}{2\pi} - \frac{\tilde{V}_{n', n_2, n_2, n'}^{(i', i_2, i_2, i')}(0)}{2\pi} \right) A_{n, n', i, i'}^+(\vec{k})|0\rangle - \sum_{n_2, i_2} v_{n_2}^{(i_2)} (\tilde{E}_{n, n_2, n, n_2}^{(i, i_2, i, i_2)}(0) - \tilde{E}_{n', n_2, n', n_2}^{(i', i_2, i', i_2)}(0)) A_{n, n', i, i'}^+(\vec{k})|0\rangle \\ - (v_n^{(i)} - v_{n'}^{(i')}) \sum_{\substack{n_1, n_4 \\ i_1, i_4}} \frac{\tilde{V}_{n_1, n', n, n_4}^{(i, i', i, i_4)}(\vec{k})}{2\pi} A_{n_1, n_4, i_1, i_4}^+(\vec{k})|0\rangle + (v_n^{(i)} - v_{n'}^{(i')}) \sum_{\substack{n_1, n_2 \\ i_1, i_2}} \tilde{E}_{n', n_1, n, n_2}^{(i', i_1, i, i_2)}(\vec{k}) A_{n_1, n_2, i_1, i_2}^+(\vec{k})|0\rangle, \quad (26)$$

where

$$\tilde{E}_{n_1, n_2, n_3, n_4}^{(i_1, i_2, i_3, i_4)}(\vec{k}) = \int \frac{d^2\vec{q}}{(2\pi)^2} \tilde{V}_{n_1, n_2, n_3, n_4}^{(i_1, i_2, i_3, i_4)}(\vec{q}) e^{i a_B^2 [\vec{q} \times \vec{k}]_z}. \quad (27)$$

The first and the second terms in Eq. (26) describe the difference between the corrections to the LL energies of the excited electron and hole, as calculated in the Hartree-Fock approximation. They define the ‘‘direct’’ and exchange interaction of the excited quasiparticle pair with the 2DEG. The third term describes a direct Coulomb interaction between the electron and the hole. The fourth term in this equation is for the nonlocal exchange interaction of the excited electron and hole. As seen from Eq. (26), the e-e interaction causes mixing of possible single-exciton states in a 2D system.

Let us now consider the details of spin-wave excitation due to the electron transition from LL (n_F, a) to the level $(n_F - 1, b)$ (see Fig. 1 and Figs. 1–3 in Ref. 48), where $(n_F - 1, b)$ and (n_F, a) are the adjacent spin-split LLs crossed with the Fermi level. It is obvious that such a transition will be possible for the filling factor $v_{n_F-1}^{(b)} < 1$ only. Assuming the energies of LLs (n_F, a) and $(n_F - 1, b)$ calculated in the Hartree approximation,^{47,48} we omit the first term in Eq. (26) because it has already been included via $-e\varphi_{e-e}$ in the definition for $E_{n_F}^{(a)}$ and $E_{n_F-1}^{(b)}$.

Since the cyclotron energy is much higher than the Zeeman splitting of LLs (see Fig. 1), all excitations other than SW lie considerably above the energy region of the spin-wave, hence, they can be neglected. Using the polar coordinate system, we can simplify Eq. (26) to have the spin exciton energy $E_{\text{SW}}(\vec{k})$ in the form:

$$E_{\text{SW}}(\vec{k}) = E_{n_F-1}^{(b)} - E_{n_F}^{(a)} + \Delta_{\text{SW}}^{(e-e)}(k), \\ \Delta_{\text{SW}}^{(e-e)}(k) = [v_{n_F-1}^{(b)} - v_{n_F}^{(a)}] \tilde{E}_{n_F, n_F-1, n_F-1, n_F}^{(a, b, b, a)}(k) \\ - [v_{n_F-1}^{(b)} - v_{n_F}^{(a)}] \frac{\tilde{V}_{n_F, n_F-1, n_F, n_F-1}^{(a, b, a, b)}(k)}{2\pi} - \\ - \sum_{n_2, i_2} v_{n_2}^{(i_2)} [\tilde{E}_{n_F-1, n_2, n_F-1, n_2}^{(b, i_2, b, i_2)}(0) - \tilde{E}_{n_F, n_2, n_F, n_2}^{(a, i_2, a, i_2)}(0)], \quad (28)$$

where

$$\tilde{E}_{n_F, n_F-1, n_F-1, n_F}^{(a, b, b, a)}(k) = \int_0^\infty \frac{qdq}{2\pi} \int_{-\infty}^{+\infty} dz_1 \int_{-\infty}^{+\infty} dz_2 e^{-q^2 a_B^2 / 2} \tilde{L}_{n_F, n_F}^{(a, a)}(z_1, z_2)$$

$$\times \left(\frac{q^2 a_B^2}{2}, z_1, z_1 \right) \tilde{D}(q, z_1, z_2) \tilde{L}_{n_F-1, n_F-1}^{(b, b)}(z_2, z_2) \\ \times \left(\frac{q^2 a_B^2}{2}, z_2, z_2 \right) J_0(k q a_B^2) \quad (29)$$

and

$$\tilde{V}_{n_F, n_F-1, n_F, n_F-1}^{(a, b, a, b)}(k) = -e^{-k^2 a_B^2 / 2} \int_{-\infty}^{+\infty} dz_1 \int_{-\infty}^{+\infty} dz_2 \tilde{L}_{n_F, n_F-1}^{(a, b)}\left(\frac{k^2 a_B^2}{2}, z_1, z_1\right) \\ \times \tilde{D}(k, z_1, z_2) \frac{k^2}{2} \tilde{L}_{n_F-1, n_F}^{(b, a)}\left(\frac{k^2 a_B^2}{2}, z_2, z_2\right). \quad (30)$$

In Eqs. (29) and (30), $J_0(x)$ is the modified zero-order Bessel function. The absorption energy and the g factor measured in ESR are determined by the long-wave energy limit of the excited spin waves:

$$E_{\text{ESR}} = E_{n_F-1}^{(b)} - E_{n_F}^{(a)} + \Delta_{\text{SW}}^{(e-e)}(0), \\ g_{\text{ESR}} = g_{(1e)} + \frac{\Delta_{\text{SW}}^{(e-e)}(0)}{\mu_B B}, \quad (31)$$

where $g_{(1e)}$ is the single-electron g factor calculated within the Hartree approximation.^{47,48} Further, we will regard the g factor in its absolute value.

C. The parabolic subband case

Consider the limiting case of the parabolic dispersion law *in the absence of SOI* for the energy of a spin wave. By changing the eight-component wave function (11) for the wave function in the parabolic subband:

$$\Psi_{n, k}^{(i)}(\vec{r}, z) \rightarrow \tilde{c}(z) \sigma_z |n, k\rangle,$$

we have the transformation

$$\tilde{L}_{n, n'}^{(i, i')}\left(\frac{q^2 a_B^2}{2}, z, z\right) \rightarrow \delta_{i, i'} |\tilde{c}(z)|^2 \begin{cases} \sqrt{\frac{n!}{n'}} L_{n'}^{n-n'}\left(\frac{q^2 a_B^2}{2}\right), & n \geq n', \\ \sqrt{\frac{n!}{n'}} L_n^{n'-n}\left(\frac{q^2 a_B^2}{2}\right), & n < n' \end{cases} \quad (32)$$

in Eqs. (29) and (30). As a result, the difference in the exchange energies of *fully filled* spin-split LLs is zero, and the expression for $\Delta_{\text{SW}}^{(e-e)}(k)$ in the parabolic subband takes the form:

$$\begin{aligned} \Delta_{\text{SW}}^{(e-e)}(k) &= (v_{n_F}^{(\uparrow)} - v_{n_F}^{(\downarrow)}) \int_0^\infty \frac{q dq}{2\pi} \tilde{V}_{\text{parabolic}}(q) e^{-q^2 a_B^2/2} \\ &\quad \times L_{n_F}^0 \left(\frac{q^2 a_B^2}{2} \right) L_{n_F}^0 \left(\frac{q^2 a_B^2}{2} \right) [1 - J_0(kq a_B^2)], \\ \tilde{V}_{\text{parabolic}}(q) &= \int_{-\infty}^{+\infty} dz_1 \int_{-\infty}^{+\infty} dz_2 \tilde{D}(k, z_1, z_2) |\tilde{c}(z_1)|^2 |\tilde{c}(z_2)|^2. \end{aligned} \quad (33)$$

When changing notations $(n_F - 1, b)$ for (n_F, \uparrow) and (n_F, a) for (n_F, \downarrow) in Eq. (33), we took into account the g factor being negative in the InAs/AlSb QW. By neglecting effects of the electrostatic imaging forces and using relation

$$\tilde{D}(q, z_1, z_2) = \frac{2\pi e^2}{q\epsilon} \quad (34)$$

for the Coulomb Green function, where ϵ is a permittivity of InAs, we arrive at an expression for the energy of a spin exciton at zero LL in the form

$$\begin{aligned} \Delta_{\text{SW}}^{(e-e)}(k) &= [v_{n_F}^{(\uparrow)} - v_{n_F}^{(\downarrow)}] \\ &\quad \times \sqrt{\frac{\pi}{2}} \frac{e^2}{\epsilon a_B} \left[1 - J_0 \left(\frac{k^2 a_B^2}{4} \right) e^{-k^2 a_B^2/4} \right]. \end{aligned} \quad (35)$$

Equation (35) coincides with that for the energy of a spin wave at a zero LL, obtained within the Hartree-Fock approximation.^{1-3,7} It should be noted that, according to the Larmor theorem, the e-e interaction produces no effect on the energy of spin resonance in the absence of SOI.

III. RESULTS AND DISCUSSIONS

To obtain the LL energies and single-electron wave functions $\Psi_{n,k}^{(i)}(\vec{r}, z)$, we solve the set of Eqs. (7)–(10) self-consistently by using an iterative procedure. To diagonalize the Hamiltonian $\hat{H}_{(1e)}$ at the $(m + 1)$ th interaction, the scattering matrix method with the wave functions found at the m th iteration is used.^{28,47} For the envelope wave function zeroth-order approximation, we picked the states in a rectangular QW. At the final iteration, we calculate the single-electron spin splitting at the Fermi level $E_{n_F-1}^{(b)} - E_{n_F}^{(a)}$ and the matrix elements $\tilde{V}_{n_1, n_2, n_3, n_4}^{(i_1, i_2, i_3, i_4)}(\vec{k})$ and $\tilde{E}_{n_1, n_2, n_3, n_4}^{(i_1, i_2, i_3, i_4)}(\vec{k})$.

The results of the calculations of single-electron LLs (n, i) in a 15-nm-wide InAs/AlSb QW in the absence of a “built-in” electric field are shown in Fig. 1. The QW material parameters used in the calculations are provided in Refs. 47 and 56.

In the calculations of spin-wave dispersion and spin resonance energies in InAs/AlSb QW heterostructures, we consider two cases: the symmetric ($n_L = n_R$) and asymmetric ($n_R = 0$) QW profiles. When the InAs/AlSb QW profile is asymmetric, the only possible “suppliers” of electrons in the QW to be taken into account are ionized surface donors in the GaSb cap layer.^{38,40} The calculations presented in this section were performed for three typical values of 2DEG concentration n_S in InAs/AlSb heterostructures with a 15-nm-wide QW having one filled electronic

subband:^{19-21,34,38,39,64,65} 2×10^{11} , 5×10^{11} , and 9×10^{11} cm^{-2} . At such 2DEG concentrations, the values of the BR spin splitting with the Fermi wave vector in asymmetric InAs/AlSb QW are 0.29, 1.10, and 2.04 meV, respectively.²⁸

A. Electron spin resonance

Figure 2 illustrates the ESR absorption energy calculations versus magnetic field in InAs/AlSb heterostructures with a 15 nm wide QW for different values of the 2DEG concentration. Black and brown curves correspond to the “single-electron” Hartree approximation in a symmetric and asymmetric QW. Red and blue curves are for the ESR absorption energies calculated with allowance for the e-e interaction in QW with a symmetric and asymmetric profiles, respectively. The arrows indicate the magnetic field values corresponding to the even-valued filling factors of LLs.

First, we analyze the single-electron energies of the spin resonance, calculated within the Hartree approximation. The features observed at even-valued filling factors of the LLs appear due to the electronic subband nonparabolicity in InAs/AlSb QW. As the magnetic field increases, the Fermi level “jumps” from one pair of spin-split LLs to the lower-lying pair with a greater spin splitting (see, e.g., Fig. 1 and Figs. 1–3 in Ref. 48). This causes a sharp rise of the spin-splitting energy at the Fermi level, followed by an abrupt change in the ESR energy. It is seen that the single-electron ESR energy in a symmetric quantum well is determined by the Zeeman splitting of LLs, demonstrating a linear dependence on magnetic field in the region of weak magnetic fields.

The BR spin splitting in an asymmetric QW leads to distortion of the monotonic dependence of single-electron ESR energy on magnetic field and appearance of a pronounced minimum in the low magnetic fields region (see Fig. 2). In this case, the spin splitting at the Fermi level is determined by two contributors: the BR- and the Zeeman splitting.³⁰⁻³² As the magnetic field increases from zero, the ESR energy quickly drops, going smoothly over to the Zeeman splitting. Note that for high LL indices n (in weak magnetic fields), the single-electron ESR energies can be obtained analytically:^{14,66}

$$E_{\text{ESR}} \approx [(\hbar\omega_c + |g_{(1e)}|\mu_B B)^2 + \Delta_R^2]^{1/2} - \hbar\omega_c, \quad (36)$$

where Δ_R is the BR splitting at the Fermi wave vector in a zero magnetic field. Thus the single-electron ESR energy decreases linearly with B in weak magnetic fields.

Strong SOI in the InAs/AlSb QWs and the nonparabolicity of electronic subbands lead to violation of the Larmor theorem applicability conditions in both symmetric (red curves) and asymmetric (blue curves) QW. The e-e interaction in narrow-gap QW causes considerable enhancement of the ESR energy, which at low magnetic fields is more than twice its single-electron value. The BR spin splitting related to the QW profile asymmetry produces a noticeable effect on the “many-particle” ESR energy in weak magnetic fields only. For strong fields, the blue and red curves in Fig. 2 have a slight difference. Note that the observed exchange enhancement of the ESR energy occurs due to the difference in the spatial structures of wave functions $\Psi_{n_F-1,k}^{(b)}(\vec{r}, z)$ and $\Psi_{n_F,k}^{(a)}(\vec{r}, z)$ for the electrons at spin-split LLs

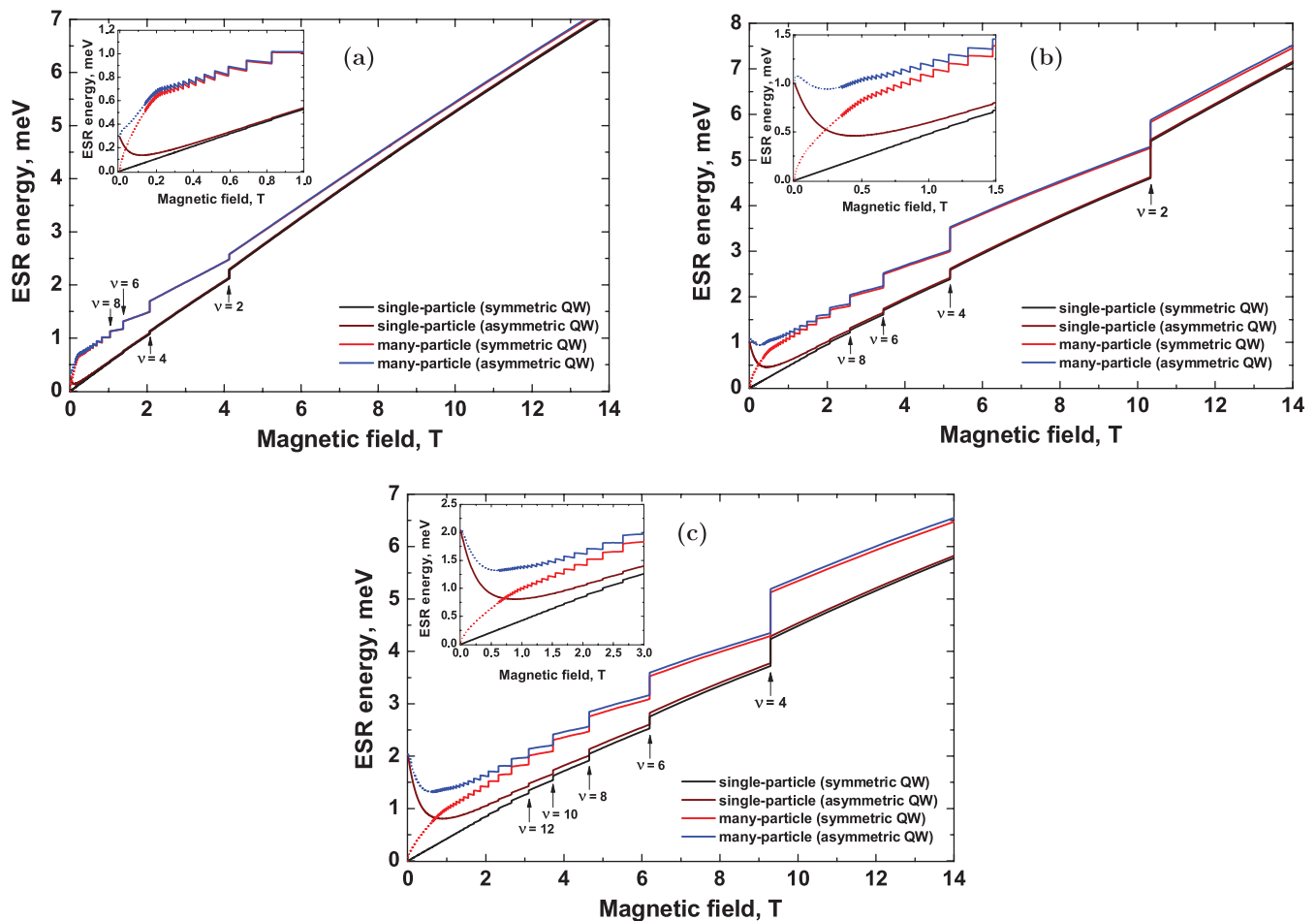


FIG. 2. (Color online) ESR energy in a 15-nm-wide InAs/AlSb QW with symmetric and asymmetric profile vs magnetic field, calculated for different 2DEG concentrations: (a) 2×10^{11} , (b) 5×10^{11} , and (c) 9×10^{11} cm^{-2} . Red and blue dotted curves correspond to the low-field values interpolated using Eqs. (36) and (37). The insets show the results of calculations in weak magnetic fields.

$(n_F - 1, b)$ and (n_F, a) ⁴⁹ resulted from the mixing between the Γ_6 , Γ_7 , and Γ_8 bands.

At low magnetic fields, estimation of the “many-electron” ESR energies involves certain technical problems, as the large number of filled LLs makes numerical calculations a particularly time-consuming procedure. Therefore all numerical calculations are done for the case $\nu < 60$, and for weaker magnetic fields, we reduce our consideration to qualitative analysis of the dependence of many-particle ESR energy on magnetic field.

The magnetic field dependence of corrections $\Delta_{\text{sw}}^{(e-e)}$ to the ESR energy at a fixed number of LL n and spin index i can be estimated based on relations (29). For simplicity, we neglect the effects of electrostatic imaging forces and use expression $\tilde{D}(q, z, z') \sim 1/q$ for the Coulomb Green function, then we have $\tilde{E}_{n_1, n_2, n_3, n_4}^{(i_1, i_2, i_3, i_4)} \sim 1/a_B \sim \sqrt{B}$. The resulting dependence of the exchange corrections to the ESR energy at integer filling factors of the LLs has the form:

$$\Delta_{\text{sw}}^{(e-e)}(0) = \tilde{C}\sqrt{B}, \quad (37)$$

where constant \tilde{C} is independent of magnetic field and is defined by the number n and spin index i of the upper fully filled LL. So, the ESR absorption energy in narrow-gap

symmetric QW in a decreasing magnetic field tends to zero, whereas in asymmetric QW to the value of the BR spin splitting at the Fermi wave vector.

In Fig. 2, the dotted curves are the results of interpolation of the many-electron ESR energy to its zero-magnetic-field values for a symmetric (red curve) and asymmetric (blue curve) InAs/AlSb QW, that was performed using Eqs. (36) and (37). One can see that the behavior of many-electron ESR energy in asymmetric quantum wells at low magnetic fields strongly depends on a magnitude of the BR spin splitting. When the latter is weak in a zero magnetic field, the field dependence of the ESR energy is monotonically increasing [see Fig. 2(a)] with increasing of the magnetic field, whereas at high values of BR splitting [see Fig. 2(c)], we observe a monotonically decreasing curve in the region of low magnetic fields.

The spin resonance energy is conventionally described in terms of effective g factor (31). In Fig. 3, we present the calculations of g factor g_{ESR} measured at a spin resonance in narrow-gap InAs/AlSb QW versus magnetic field. Black and brown curves correspond to the “single-electron” Hartree approximation in the symmetric and asymmetric QW. Red and blue curves are based on the g -factor data obtained with account for the e-e interaction in QW with a symmetric and

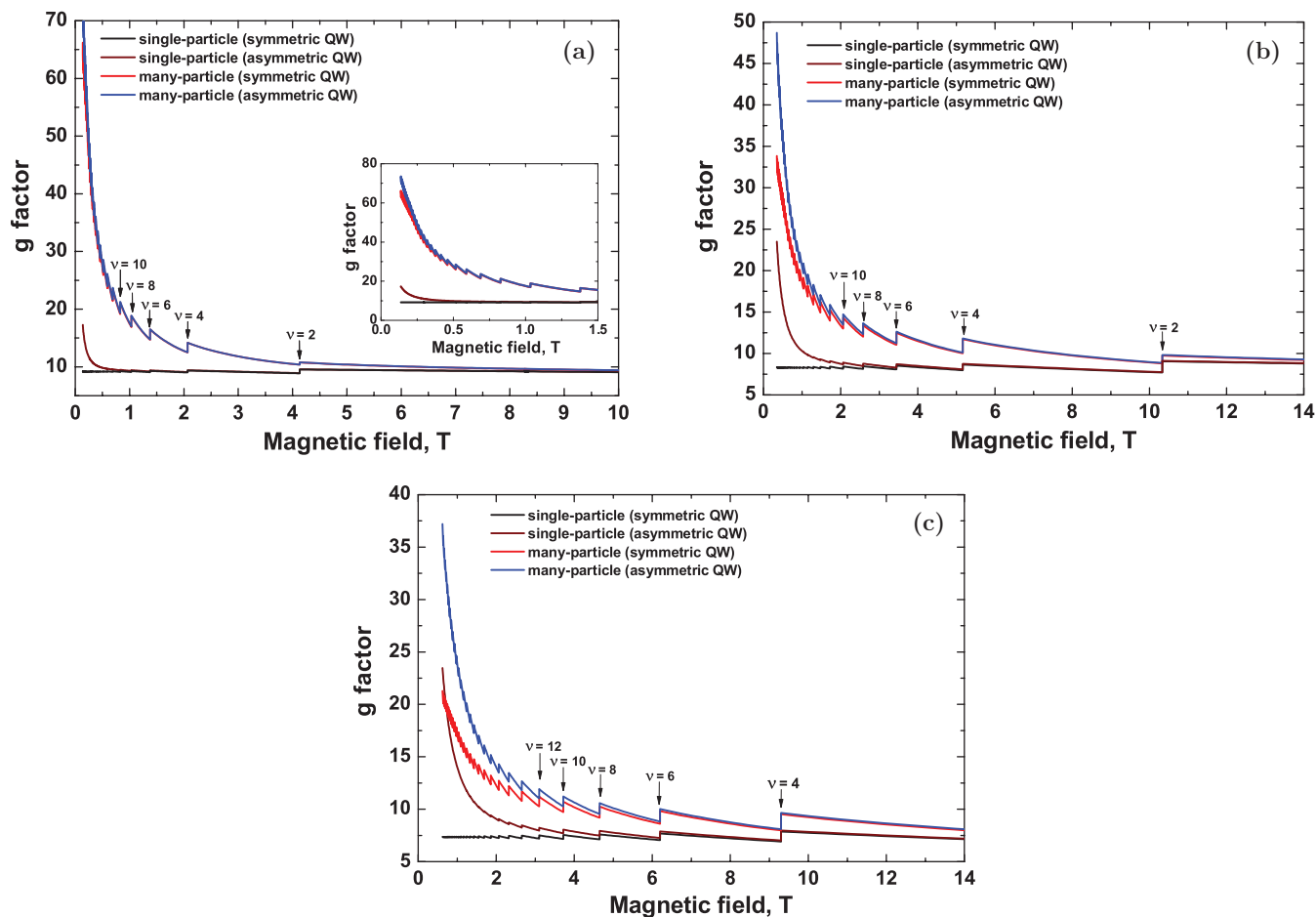


FIG. 3. (Color online) Calculated ESR g factor in a 15-nm wide InAs/AlSb QW with a symmetric and asymmetric profile as a function of magnetic field for different 2DEG concentrations: (a) $2 \times 10^{11} \text{ cm}^{-2}$, (b) $5 \times 10^{11} \text{ cm}^{-2}$, (c) $9 \times 10^{11} \text{ cm}^{-2}$. The arrows indicate the magnetic field values corresponding to even-valued filling factors of the Landau levels. The insert offers the data calculated for low magnetic fields.

asymmetric profiles, respectively. The magnetic field values corresponding to the even-valued filling factors of LLs are indicated by arrows.

It is seen that the single-electron g factor in symmetric QW (black curves in Fig. 3) under low magnetic fields is a constant depending on the 2DEG concentration; for the values 2×10^{11} , 5×10^{11} , and $9 \times 10^{11} \text{ cm}^{-2}$ it was found to be 9.2, 8.3, and 7.3 (in absolute value), respectively. At higher 2DEG concentrations, the Fermi level crosses the higher-lying pairs of LLs, being less spin-split than the pairs below, which reduce the single-electron g factor in symmetric QWs in weak magnetic fields. The effect of BR spin splitting in asymmetric QWs causes a natural divergence of $g_{(1e)}$ in a zero magnetic field (brown curves in Fig. 3).

Taking the e-e interaction in narrow-gap QWs into account, yields a considerable enhancement of g_{ESR} in both symmetric (red curves) and asymmetric (blue curves) QWs. At low magnetic fields, the square root dependence (37) for $\Delta_{\text{SW}}^{(e-e)}(0)$ leads to divergence of the many-electron ESR g factor in symmetric QWs. In asymmetric QWs, the inclusion of $\Delta_{\text{SW}}^{(e-e)}(0)$ increases the BR splitting induced divergence of the g factor under low magnetic fields. In high magnetic fields, in accordance with Eq. (37), the magnitude of the exchange enhancement of many-electron g factor g_{ESR}

decreases with a growing magnetic field, which is illustrated in Fig. 3.

The many-body ESR energy renormalization, predicted for narrow-gap n -type QWs in this paper, should also take place in each 2D system, where the single-electron energy spectrum is described by the $8 \times 8 \mathbf{k} \cdot \mathbf{p}$ Hamiltonian, since it is caused by both mixing of the Γ_6 , Γ_7 , and Γ_8 bands resulted in nondiagonal terms appearing in H_Z (6) and by SOI defined by parameter Δ in Eq. (5). However, such renormalization is absent in the model system with $H_Z = 0$ and $\Delta = 0$.⁴⁹ In 2D systems, other than n -type InAs^{19–23} and InSb^{15–18} QWs, the renormalized values of ESR energy depend not only on Δ but also on Luttinger parameters⁴¹ γ_1 , γ_2 , and γ_3 as well. Moreover, we assume that in p -type as well as in HgTe QWs,^{67–69} e-e interaction could lead not to the *enhancement* but to the *reduction* of ESR energy.

It is well known that in HgTe/CdHgTe QWs wider than a critical thickness d_c ($d > d_c$, $d_c \approx 6 \text{ nm}$), the electronic structure is inverted.^{67,68} However, for the narrow wells ($d < d_c$), the electronic states have a normal band structure of QW states, which takes place in narrow-gap QWs⁶⁹ such as InAs or InSb QWs. Therefore we expect an exchange enhancement of ESR energy in HgTe/CdHgTe QWs with $d < d_c$. In the QWs with a critical width d_c , the electronic structure is described by

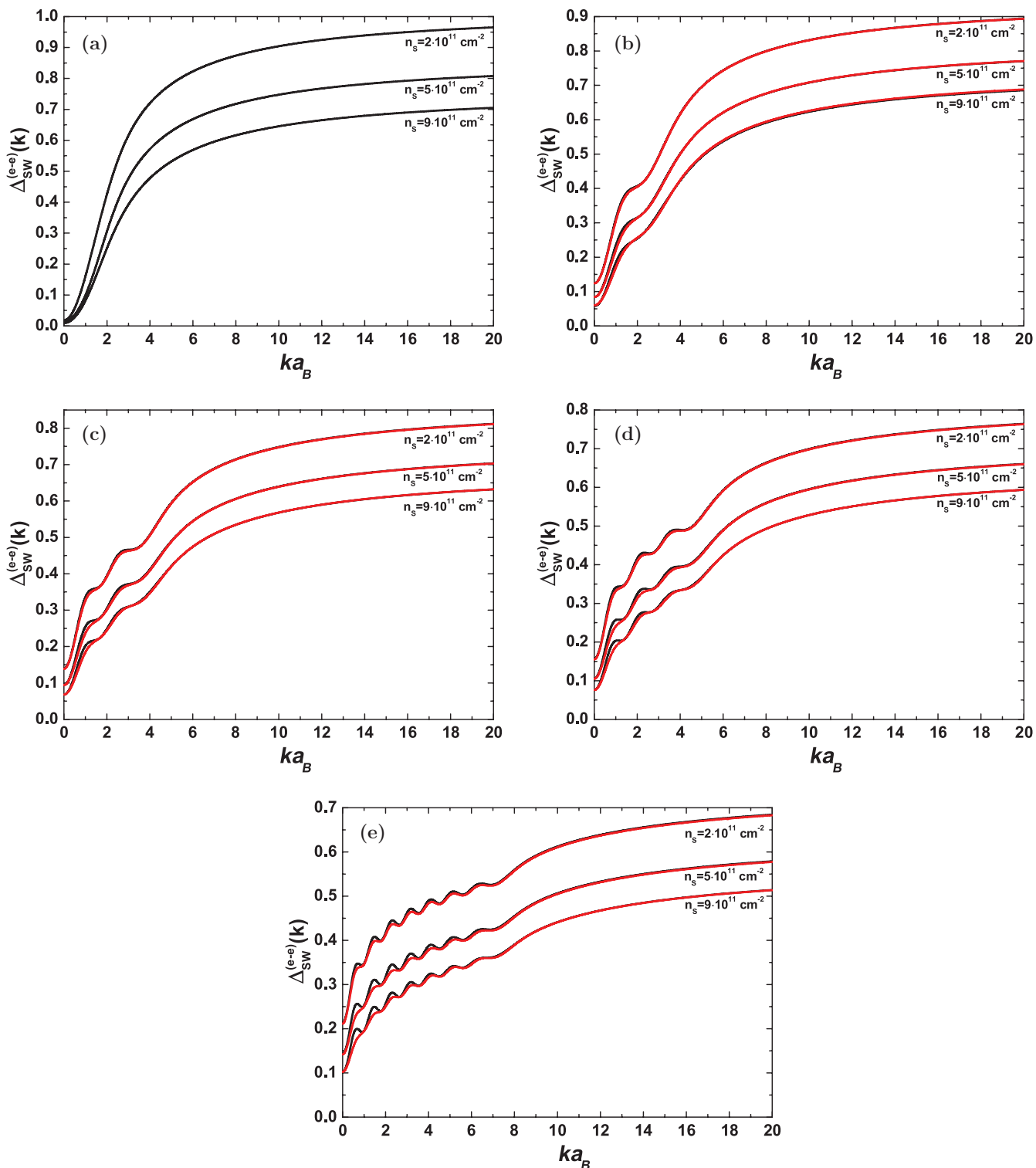


FIG. 4. (Color online) The energy of SW excitations $\Delta_{\text{SW}}^{(e-e)}(k)$ in a 15-nm InAs/AlSb QW in units of $e^2/\epsilon a_B$, counted from $g_{(1e)}\mu_B B$ at different values of 2DEG concentration for $\nu = 1$ (a), 3 (b), 5 (c), 7 (d), and 15 (e). Red curves are for the SW excitations in asymmetric QWs and black curves correspond to $\Delta_{\text{SW}}^{(e-e)}(k)$ in symmetric QWs.

a massless Dirac fermion dispersion^{67,68} as in graphene. As the Larmor theorem is valid for graphene,^{70,71} we also do not expect the many-particle renormalization of ESR energy in the HgTe/CdHgTe QWs with the critical width. Further, we explain why the reduction of ESR energy in the HgTe/CdHgTe

QWs with inverted band structure ($d > d_c$), induced by e-e interaction, is suspected.

Previously, we have demonstrated that ESR and quasi-particle g factors (measured in magnetotransport) coincide at even-valued filling factors of the LLs,⁴⁹ therefore the

enhancement/reduction of quasiparticle spin-gap at even LL filling factors is equivalent to the enhancement/reduction of ESR energy. The reduction of quasiparticle spin-gap in HgTe/CdHgTe QWs was observed by Zhang *et al.*,⁷² who extracted the values from magnetotransport measurements in tilted magnetic fields. The experimental values of quasiparticle spin gap at even LL filling factors in the QW with inverted band structure ($d > d_c$) were significantly lower than single-electron ones, while the experimental values in the HgTe/CdHgTe QWs with $d < d_c$ exceeded the single-particle spin-gap values.

We note that Zhang *et al.* completely ignored the exchange interaction effects⁵¹ in the interpretations of their experimental results, assuming these effects to be unimportant at $20 > \nu > 4$. However, according to the theory of Ando and Uemura,⁵¹ developed for 2D systems with parabolic subbands, and in accordance with our theoretical studies,^{29,47,48} in addition to the effect of parallel magnetic field component on single-electron LLs, e-e interaction should also be taken into account at all filling factors.

We stress that the above mentioned arguments are just qualitative, since our model proposed for n -type QWs based on narrow-gap semiconductors (InAs, InSb, and their alloys) are not applied for p -type QWs and HgTe QWs. The effect of e-e interaction on the ESR energy in HgTe/CdHgTe QWs will be the subject of our future research.

B. Spin-wave excitations

As mentioned in Introduction, in a 2DEG with rotational invariance in the spin space the e-e interactions do not change the spin-wave excitation energy at $k = 0$, and the SW energy reaches the unshifted Zeeman energy in the long-wavelength limit, as required by the Larmor theorem. In the previous section, we have demonstrated the Larmor theorem violation in narrow-gap QWs with a symmetric and asymmetric energy profile. Here, we address the dispersion of spin waves in narrow-gap InAs/AlSb QWs.

Figure 4 presents the results of calculations of spin wave energy $\Delta_{\text{SW}}^{(e-e)}(k)$ (in units of $e^2/\epsilon a_B$) at odd-valued filling factors of the LLs ($\nu = 1, 3, 5, 7, 15$) in the 15-nm-wide InAs/AlSb QWs for different values of 2DEG concentration. The energy was counted from the single-electron values of the ESR energy $g_{(1e)}\mu_B B$. Black curves correspond to the symmetric QW data, red curves are for the asymmetric QW data obtained with allowance for the BR spin splitting. The numbers under the curves are the values of 2DEG concentration.

For $\nu = 1$, the red and blue curves coincide at fixed concentration values, i.e., the BR spin splitting in quantizing magnetic fields has practically no effect on the spin waves dispersion law. It is seen that the nonparabolicity of electronic subbands in narrow-gap QWs makes the energy of spin waves dependent on a 2DEG concentration. Note that, in accordance with Eq. (35), in QW with the parabolic subbands given fixed filling factors the value of does not depend on 2DEG concentration. The shape of the curves in Fig. 4(a) is in a “qualitative agreement” with the spin waves dispersion law at $\nu = 1$ in the parabolic subbands QWs [see Eq. (35)]. With a growing value of the LL filling factors, the BR spin splitting influence on the energy of SW excitations increases [see Figs. 4(b)–4(e)]. The biggest difference in the dispersion

laws for the spin waves in symmetric and asymmetric QWs is observed in the range of small values ka_B .

Another remarkable feature of the SW dispersion law in narrow-gap QW, besides the $\Delta_{\text{SW}}^{(e-e)}(k)$ dependence on n_S , is that the spin waves have a gap at $k = 0$. The gap appears in the SW-excitations spectrum through violation of the Larmor theorem in narrow-gap QWs because of both SOI and subband nonparabolicity induced by the mixing between the conduction and valence bands. It also leads to exchange enhancement of the ESR g factor (see Sec. III A). One can see that the gap increases with a lowering concentration of 2DEG and/or at higher values of the LL filling factor. In vicinity of $k = 0$, the spin wave dispersions are determined by two terms: Eq. (29), quadratic in k , and by Eq. (30), which is linear in the wave vector, in contrast to the QW with the parabolic subbands, where the spin waves have a quadratic dispersion law in the long wave-length limit. In the limit of infinitely large wave vectors, a spin wave splits into two noninteracting quasiparticles whose energy does not depend on k , being determined by the “unscreened” exchange interaction of the excited electron and hole with the 2DEG [see Eq. (28)].

IV. CONCLUSIONS

We have studied the spin-wave excitations and the electron spin resonance in a perpendicular magnetic field in narrow-gap QWs with symmetric and asymmetric energy profiles. In the calculations, we have taken into account the subband nonparabolicity, lattice-mismatch deformation, spin-orbit interaction, and e-e interaction in the Hartree-Fock approximation by using the eight-band $\mathbf{k}\cdot\mathbf{p}$ Hamiltonian. A significant enhancement of the ESR energy through exchange interaction in symmetric and asymmetric QWs, and the exchange-induced divergence of the ESR g factor in symmetric QWs in weak magnetic field have been demonstrated. It was also shown that the nonmonotonic dependence of ESR energy in narrow-gap asymmetric QWs in weak magnetic fields is determined by both the BR spin splitting and the e-e interaction. The calculations performed for InAs/AlSb QW heterostructures have exposed a gap in the long-wavelength part of the SW-excitation energy spectrum, whose value depends on a 2DEG concentration in narrow-gap QWs. The obtained results indicate a significant influence of both e-e interaction and Bychkov-Rashba spin splitting on ESR in narrow-gap QW heterostructures and in any case should be taken into consideration in interpreting the experimental data. Unfortunately, there are currently no data available in literature on the experimental studies of ESR in narrow-gap QWs in perpendicular (*not tilted*, cf. Refs. 15 and 16) magnetic fields. We hope that our results will stimulate further research on the ESR and inelastic light scattering in narrow-gap QW heterostructures in perpendicular magnetic fields.

ACKNOWLEDGMENTS

This work is partially supported by the Russian Foundation for Basic Research (Grants 11-02-93111, 12-02-00940, 13-02-00894), by the Russian Academy of Sciences, and by Russian Ministry of Education and Science (Grant HIII-4756.2012.2). S.S. Krishtopenko is grateful to the nonprofit Dynasty Foundation for financial support.

*gavr@ipmras.ru

†michel.goiran@lncmi.cnrs.fr

- ¹C. Kallin and B. I. Halperin, *Phys. Rev. B* **30**, 5655 (1984).
- ²D. Antoniou and A. H. MacDonald, *Phys. Rev. B* **43**, 11686 (1991).
- ³J. P. Longo and C. Kallin, *Phys. Rev. B* **47**, 4429 (1993).
- ⁴T. Nakajima and H. Aoki, *Phys. Rev. Lett.* **73**, 3568 (1994).
- ⁵J. K. Jain, *Phys. Rev. Lett.* **63**, 199 (1989).
- ⁶G. Murthy, *Phys. Rev. B* **60**, 13702 (1999).
- ⁷S. S. Mandal, *Phys. Rev. B* **56**, 7525 (1997).
- ⁸A. Pinczuk, B. S. Dennis, D. Heiman, C. Kallin, L. Brey, C. Tejedor, S. Schmitt-Rink, L. N. Pfeiffer, and K. W. West, *Phys. Rev. Lett.* **68**, 3623 (1992).
- ⁹M. Dobers, K. v. Klitzing, and G. Weimann, *Phys. Rev. B* **38**, 5453 (1988).
- ¹⁰Y. A. Nefyodov, A. V. Shchepetilnikov, I. V. Kukushkin, W. Dietsche, and S. Schmult, *Phys. Rev. B* **83**, 041307 (2011).
- ¹¹Y. A. Nefyodov, A. V. Shchepetilnikov, I. V. Kukushkin, W. Dietsche, and S. Schmult, *Phys. Rev. B* **84**, 233302 (2011).
- ¹²Y. A. Nefyodov, A. A. Fortunatov, A. V. Shchepetilnikov, and I. V. Kukushkin, *JETP Lett.* **91**, 357 (2010).
- ¹³M. Califano, T. Chakraborty, P. Pietiläinen, and C.-M. Hu, *Phys. Rev. B* **73**, 113315 (2006).
- ¹⁴Y. A. Bychkov and E. I. Rashba, *J. Phys. C: Solid State Phys.* **17**, 6039 (1984).
- ¹⁵G. A. Khodaparast, D. C. Larrabee, J. Kono, D. S. King, S. J. Chung, and M. B. Santos, *Phys. Rev. B* **67**, 035307 (2003).
- ¹⁶G. A. Khodaparast, R. C. Meyer, X. H. Zhang, T. Kasturirachchi, R. E. Doezema, S. J. Chung, N. Goel, M. B. Santos, and Y. J. Wang, *Physica E* **20**, 386 (2004).
- ¹⁷Y. B. Vasilyev, F. Gouider, G. Nachtwei, and P. D. Buckle, *Semiconductors* **44**, 1511 (2010).
- ¹⁸F. Gouider, Y. B. Vasilyev, M. Bugár, J. Könemann, P. D. Buckle, and G. Nachtwei, *Phys. Rev. B* **81**, 155304 (2010).
- ¹⁹M. J. Yang, R. J. Wagner, B. V. Shanabrook, J. R. Waterman, and W. J. Moore, *Phys. Rev. B* **47**, 6807 (1993).
- ²⁰M. J. Yang, P. J. Lin-Chung, B. V. Shanabrook, J. R. Waterman, R. J. Wagner, and W. J. Moore, *Phys. Rev. B* **47**, 1691 (1993).
- ²¹V. Y. Aleshkin, V. I. Gavrilenko, A. V. Ikonnikov, Y. G. Sadofyev, J. P. Bird, S. R. Johnson, and Y. H. Zhang, *Semiconductors* **39**, 62 (2005).
- ²²A. V. Ikonnikov, S. S. Krishtopenko, V. I. Gavrilenko, Y. G. Sadofyev, Y. B. Vasilyev, M. Orlita, and W. Knap, *J. Low Temp. Phys.* **159**, 197 (2010).
- ²³S. S. Krishtopenko, A. V. Ikonnikov, A. V. Maremyanin, K. E. Spirin, V. I. Gavrilenko, Y. G. Sadofyev, M. Goiran, M. Sadowsky, and Y. B. Vasilyev, *J. Appl. Phys.* **111**, 093711 (2012).
- ²⁴G. A. Khodaparast, R. E. Doezema, S. J. Chung, K. J. Goldammer, and M. B. Santos, *Phys. Rev. B* **70**, 155322 (2004).
- ²⁵A. M. Gilbertson, W. R. Branford, M. Fearn, L. Buckle, P. D. Buckle, T. Ashley, and L. F. Cohen, *Phys. Rev. B* **79**, 235333 (2009).
- ²⁶M. A. Leontiadou, K. L. Litvinenko, A. M. Gilbertson, C. R. Pidgeon, W. R. Branford, L. F. Cohen, M. Fearn, T. Ashley, M. T. Emeny, B. N. Mordin *et al.*, *J. Phys.: Condens. Matter* **23**, 035801 (2011).
- ²⁷J. P. Heida, B. J. van Wees, J. J. Kuipers, T. M. Klapwijk, and G. Borghs, *Phys. Rev. B* **57**, 11911 (1998).
- ²⁸V. I. Gavrilenko, S. S. Krishtopenko, and M. Goiran, *Semiconductors* **45**, 110 (2011).
- ²⁹S. S. Krishtopenko, K. P. Kalinin, V. I. Gavrilenko, Y. G. Sadofyev, and M. Goiran, *Semiconductors* **46**, 1163 (2012).
- ³⁰P. Pfeffer and W. Zawadzki, *Phys. Rev. B* **52**, R14332 (1995).
- ³¹P. Pfeffer and W. Zawadzki, *Phys. Rev. B* **59**, R5312 (1999).
- ³²W. Zawadzki and P. Pfeffer, *Semicond. Sci. Technol.* **19**, R1 (2004).
- ³³G. Dresselhaus, *Phys. Rev.* **100**, 580 (1955).
- ³⁴V. Y. Aleshkin, V. I. Gavrilenko, A. V. Ikonnikov, S. S. Krishtopenko, Y. G. Sadofyev, and K. E. Spirin, *Semiconductors* **42**, 828 (2008).
- ³⁵G. Tuttle, H. Kroemer, and J. H. English, *J. Appl. Phys.* **65**, 5239 (1989).
- ³⁶G. Tuttle, H. Kroemer, and J. H. English, *J. Appl. Phys.* **67**, 3032 (1990).
- ³⁷C. Gauer, J. Scriba, A. Wixforth, J. P. Kotthaus, C. Nguyen, G. Tuttle, J. H. English, and H. Kroemer, *Semicond. Sci. Technol.* **8**, S137 (1993).
- ³⁸V. I. Gavrilenko, A. V. Ikonnikov, S. S. Krishtopenko, A. A. Lastovkin, K. V. Maremyanin, Y. G. Sadofyev, and K. E. Spirin, *Semiconductors* **44**, 616 (2010).
- ³⁹V. Y. Aleshkin, V. I. Gavrilenko, D. M. Gaponova, A. V. Ikonnikov, K. V. Maremyanin, S. V. Morozov, Y. G. Sadofyev, S. R. Johnson, and Y.-H. Zhang, *Semiconductors* **39**, 22 (2005).
- ⁴⁰K. E. Spirin, K. P. Kalinin, S. S. Krishtopenko, K. V. Maremyanin, V. I. Gavrilenko, and Y. G. Sadofyev, *Semiconductors* **46**, 1396 (2012).
- ⁴¹E. G. Novik, A. Pfeuffer-Jeschke, T. Jungwirth, V. Latussek, C. R. Becker, G. Landwehr, H. Buhmann, and L. W. Molenkamp, *Phys. Rev. B* **72**, 035321 (2005).
- ⁴²B. A. Foreman, *Phys. Rev. B* **56**, R12748 (1997).
- ⁴³R. Winkler, *Surf. Sci.* **361/362**, 411 (1996).
- ⁴⁴R. Winkler, *Spin Orbit Coupling Effects in Two-Dimensional Electron and Hole Systems* (Springer, Berlin, Heidelberg, 2003).
- ⁴⁵J. Scriba, A. Wixforth, J. Kotthaus, C. Bolognesi, C. Nguyen, and H. Kroemer, *Solid State Commun.* **86**, 633 (1993).
- ⁴⁶P. Pfeffer and W. Zawadzki, *Phys. Rev. B* **68**, 035315 (2003).
- ⁴⁷S. S. Krishtopenko, V. I. Gavrilenko, and M. Goiran, *J. Phys.: Condens. Matter* **23**, 385601 (2011).
- ⁴⁸S. S. Krishtopenko, V. I. Gavrilenko, and M. Goiran, *J. Phys.: Condens. Matter* **24**, 135601 (2012).
- ⁴⁹S. S. Krishtopenko, V. I. Gavrilenko, and M. Goiran, *J. Phys.: Condens. Matter* **24**, 252201 (2012).
- ⁵⁰S. S. Krishtopenko, V. I. Gavrilenko, and M. Goiran, *Solid State Phenomena* **190**, 554 (2012).
- ⁵¹T. Ando and Y. Uemura, *J. Phys. Soc. Jpn.* **37**, 1044 (1974).
- ⁵²S. S. Krishtopenko, *J. Phys.: Condens. Matter* **25**, 105601 (2013).
- ⁵³S. D. Ganichev, V. V. Bel'kov, L. E. Golub, E. L. Ivchenko, P. Schneider, S. Giglberger, J. Eroms, J. De Boeck, G. Borghs, W. Wegscheider *et al.*, *Phys. Rev. Lett.* **92**, 256601 (2004).
- ⁵⁴S. Giglberger, L. E. Golub, V. V. Bel'kov, S. N. Danilov, D. Schuh, C. Gerl, F. Rohlffing, J. Stahl, W. Wegscheider, D. Weiss *et al.*, *Phys. Rev. B* **75**, 035327 (2007).
- ⁵⁵I. Semenikhin, A. Zakharova, and K. A. Chao, *Phys. Rev. B* **77**, 113307 (2008).
- ⁵⁶I. Vurgaftman, J. R. Meyer, and L. R. Ram-Mohan, *J. Appl. Phys.* **89**, 5815 (2001).
- ⁵⁷S. Dickmann and S. Iordanskii, *JETP Lett.* **63**, 50 (1996).
- ⁵⁸S. Dickmann and S. Iordanskii, *JETP Lett.* **70**, 543 (1999).
- ⁵⁹Y. A. Bychkov and G. Martinez, *Phys. Rev. B* **66**, 193312 (2002).
- ⁶⁰S. Dickmann, V. Zhilin, and D. Kulakovskii, *JETP* **101**, 892 (2005).

- ⁶¹S. Dickmann and I. V. Kukushkin, *Phys. Rev. B* **71**, 241310 (2005).
- ⁶²Y. A. Bychkov and G. Martinez, *Phys. Rev. B* **72**, 195328 (2005).
- ⁶³S. Dickmann and T. Ziman, *Phys. Rev. B* **85**, 045318 (2012).
- ⁶⁴Y. G. Sadofyev, A. Ramamoorthy, B. Naser, J. P. Bird, S. R. Johnson, and Y.-H. Zhang, *Appl. Phys. Lett.* **81**, 1833 (2002).
- ⁶⁵J. Shen, J. D. Dow, S. Y. Ren, S. Tehrani, and H. Goronkin, *J. Appl. Phys.* **73**, 8313 (1993).
- ⁶⁶B. Das, S. Datta, and R. Reifenberger, *Phys. Rev. B* **41**, 8278 (1990).
- ⁶⁷B. A. Bernevig, T. L. Hughes, and S.-C. Zhang, *Science* **314**, 1757 (2006).
- ⁶⁸M. König, S. Wiedmann, C. Brüne, A. Roth, H. Buhmann, L. W. Molenkamp, X.-L. Qi, and S.-C. Zhang, *Science* **318**, 766 (2007).
- ⁶⁹M. Zholudev, F. Teppe, M. Orlita, C. Consejo, J. Torres, N. Dyakonova, M. Czapkiewicz, J. Wróbel, G. Grabecki, N. Mikhailov *et al.*, *Phys. Rev. B* **86**, 205420 (2012).
- ⁷⁰R. Roldán, J.-N. Fuchs, and M. O. Goerbig, *Phys. Rev. B* **82**, 205418 (2010).
- ⁷¹R. G. Mani, J. Hankinson, C. Berger, and W. A. de Heer, *Nat. Commun.* **3**, 996 (2012).
- ⁷²X. C. Zhang, K. Ortner, A. Pfeuffer-Jeschke, C. R. Becker, and G. Landwehr, *Phys. Rev. B* **69**, 115340 (2004).